Data-driven calibration for cup anemometer at different measurement locations around buildings using transfer learning based on domain adaptation

Rongmao Li[1*], *Hideki* Kikumoto[2], and *Hongyuan* Jia[2]

[1] Graduate School of Engineering, The University of Tokyo, Tokyo, Japan
[2] Institute of Industrial Science, The University of Tokyo, Tokyo, Japan

Abstract. In recent years, high-precision sensors, e.g., ultrasonic anemometers, have been widely used for wind measurement. However, conventional sensors, e.g., cup anemometers, are yet to be replaced owing to their low-cost advantages and high robustness in an uncertain environment. Considering that data-driven calibration methods are used to improve the measurement accuracy of cup anemometers, this study proposed a transfer learning method based on domain adaptation, so that existing measurement data can be used for model training in new measurement scenarios, thus reducing the cost of secondary data collection. In summary, at the corner and side of a building in a new measurement site considered for experiments, the results of the proposed method indicated that the relative errors of pulsation parameters, e.g., the standard deviation wind speed, turbulence intensity, and gust factor, more significantly reduced compared to the conventional machine learning method.

1 Introduction

An ultrasonic anemometer (UA) can accurately capture the details of three-directional wind velocity and its fluctuating characteristics. However, inaccurate values may be captured when the UA is used in an uncertain environment (rainfall) [1]. Compared to the UA, a cup anemometer (CA) offers the advantages of low cost and high robustness. Therefore, accurate wind measurements can be efficiently performed at a low cost using a well-calibrated CA that can capture pulsating wind characteristics similar to the UA.

However, a CA possesses the disadvantages of inevitable start-up wind speed, time lag, and overspeed for mean wind speed measurement owing to the inertia caused by the weight of its components [2]. Over the past few decades, CA calibration relied on wind tunnel experiments (WTEs) to ensure the linear relationship between wind speed and rotational speed, regarded as standard calibration for wind research. However, standard calibration cannot well calibrate the non-linear response of the CA at low wind speed. Owing to mechanical properties, the calibrated CA cannot accurately capture wind fluctuation compared with the UA. Thus, an additional calibration method is required to improve the CA performance.

In recent years, the calibration of low-cost sensors has been achieved with high accuracy using machine learning [3]. For instance, with regard to the CA, Bégin-Drolet et al. (2013) [4] proposed a non-linear regression model with an artificial neural network (ANN). CA observations were set as input values in WTEs and hot-wire anemometer observations were selected as calibration targets. The results confirmed that the ANN model is an effective method. However, its effectiveness has not been verified in the actual field. Li and Kikumoto (2022) proposed a data-driven calibration CA method around buildings based on the ANN and field measurements. By fitting the measurements obtained using the CA to the UA, the wind speed statistics of the CA samplings were corrected to achieve values closer to those of the UA, and the time lag of the CA was almost excluded, which was validated at multiple observation locations [5]. However, as a drawback, the model training based on the conventional machine learning theory requires a considerable amount of training data for each prediction task. Therefore, a prolonged period of data collection and additional cost of sensors need to be considered for acquiring training data for new tasks, which is in contrast to the aim of developing a low-cost sensor calibration technique. To improve the generalization performance and efficiency of the ANN model, this study proposes a transfer learning method based on domain adaptation, so that previously collected training data can be used for model training in new calibration scenarios, thus reducing the cost of secondary data collection [6].

2 Methodology

The proposed method is similar to a field calibration method based on the principle of fitting the measurements of the CA to the UA, aiming to improve

* Corresponding author: lrm99@iis.u-tokyo.ac.jp

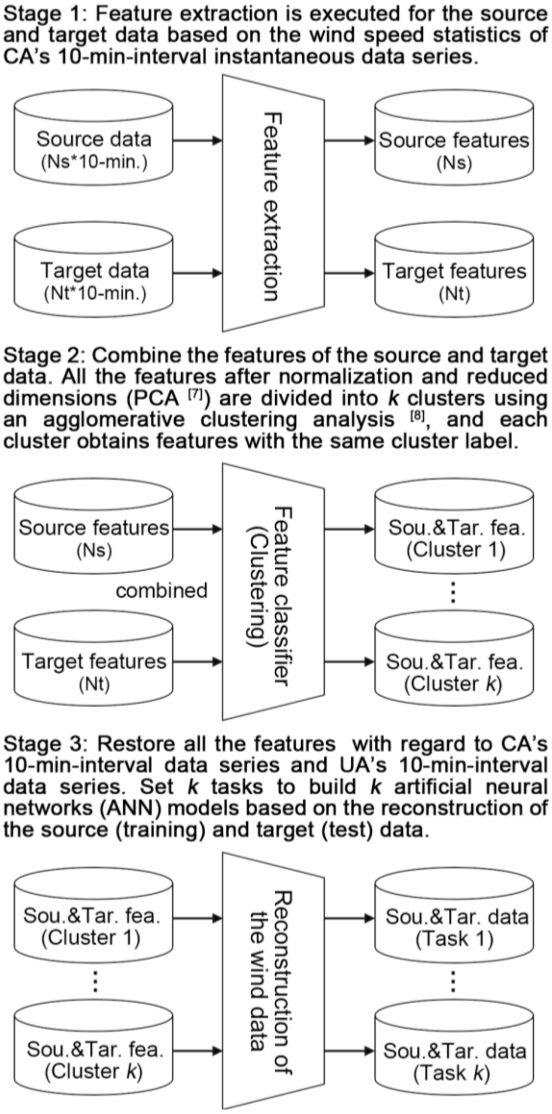

Fig. 1. Proposed domain adaptation method.

the accuracy response of the CA, i.e., closer to the UA accuracy. This method collects training (source) data from one observation site and evaluates calibration performance based on test (target) data collected from a different scenario. The conventional machine learning method uses all the source data for model training. In contrast, the proposed method selects a part of the source data based on the clustering algorithm to adapt to the target data in new tasks. In Fig. 1, three stages of the proposed method are introduced. For feature extraction in stage 1, the inputs of the clustering algorithm are the statistical features of wind speed at intervals of 10 min, rather than the whole data series, which helps realize the lightweight of the calculation load. For clustering, the agglomerative hierarchical clustering analysis based on Ward's method, which minimizes the variance of within-clusters, [8] is used in stage 2. In stage 3, features segmented in k clusters are returned to their corresponding source and target data and used for the training and prediction of ANN models for k calibration tasks. Finally, the predicted values of the k ANN models are integrated into the final calibration results.

3 Data collection

In the measurement process, the pedestrian level wind condition around buildings was considered as an application scenario in an experimental field of the Institute of Industrial Science of the University of Tokyo (Kashiwa campus, Chiba, Japan). As shown in Fig. 2(a), the first measurement at site 1 is performed in the vicinity of the test building (6 m high) to collect source data for model training. As shown in Fig. 3, the second measurement at site 2 is performed near another test building (15 m high) to collect target data for prediction. As illustrated in Fig. 2(b), two CAs (CYG-3102; named CA1 and CA2) and two UAs (CYG-81000; named UA1 and UA2) from the R. M. Young Company are adopted. UA1 and UA2 were set as the calibration targets of CA1 and CA2, respectively.

For CA1 calibration, source data were collected from the open space (OS) of site 1, and target data were collected from the corner of the building (OS*) of site 2. For CA2 calibration, source data were collected from the building side (BS) (6-m high building) of site 1, and target data were collected from another building side (BS*) (15 m high) of site 2. The difference between the source and target data of CA1 and CA2 depends on wind conditions owing to the locations and heights of the surrounding buildings.

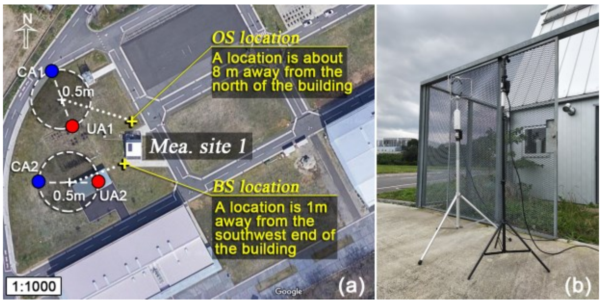

Fig. 2. Measuring system: (a) Map of the OS and BS locations at site 1. (b) Sensors: UA (left) and CA (right).

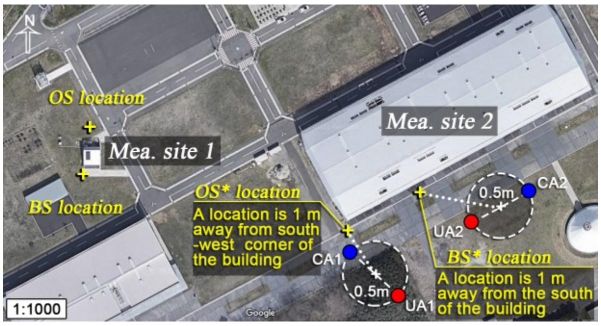

Fig. 3. Map of the OS* and BS* locations at site 2.

The UAs were installed at a horizontal distance of 0.5 m from the CAs to nearly measure the wind speed at their central location. All the UAs and CAs were installed at the same height of 1.5 m from the ground in the OS, BS, OS*, and BS* locations to measure the pedestrian-level wind. The sampling frequency of each sensor was 10 Hz. The equivalent horizontal wind speed of each UA was calculated using two horizontal wind speed components ($\sqrt{u^2 + v^2}$) to match that of each CA.

After removing the irregular data of rainy days, the raw data were calculated considering instantaneous wind data (at an interval of 3 s with regard to moving average). Finally, 1930 sets of the 10-min-interval data series were extracted from each sensor in the OS and BS locations, and 146 and 291 sets of the same data series were collected from each sensor in the OS* and BS* locations.

4 Experimental study

The experiment in this study has two goals: 1) Set the conventional machine learning method as a baseline to validate the advantage of the proposed method. 2) As critical factors affect the results of clustering analysis, determine an appropriate feature selection scheme from feature extraction with regard to the inaccuracy of the CA (Table 1) to improve the domain adaptation effect and calibration accuracy.

Table 1. Feature extraction for clustering based on the statistics of the divided10-min-interval data series of the CA.

No.	Feature
1	Mean
2	Turbulence intensity (TI)
3	Maximum value (Max)
4	Standard deviation (STD)
5	Gust factor (GF)
6	Average absolute deviation
7	Difference between maximum and minimum values
8	Median
9	Median absolute deviation
10	Interquartile range
11	Number of peaks
12	Energy

Based on Table 1, different calibration cases are set as follows:

- Case 0: Conventional machine learning method
- Case 1: Proposed method with features listed in Nos. 1 and 2
- Case 2: Proposed method with features listed in Nos. 1–5
- Case 3: Proposed method with all the 12 features

Herein, Case 0 is considered as the baseline of the proposed method. Cases 1–3 of the proposed method are used for comparing the effects of different feature selections on the results.

Table 2. Hyperparameter settings of ANN models.

Item	Setting
Hidden layer number	5
Hidden unit number	96
Loss function	Mean absolute percentage error
Active function	ReLU
Weight initializer	He Uniform
Optimization method	Adam
Learning rate	0.0003
Batch size	1024

To compare the performance of Cases 0–3, ANN models were built as unified predictors with the same hyper-parameters. The structure of the ANN models was based on the multiple-input single-output type. The CA measurements obtained within the first 3 s were set as input values to predict the true wind speed (with respect to the UA) owing to the late response of the CA. Ten percent of training data were randomly applied as validation data. The minimum and maximum values of the CA data were scaled between [0, 1]. The early stopping method was adopted to prevent overfitting, and the allowable number of steps that the validation loss does not continue to decline was set to 10. Other settings are listed in Table 2.

5 Results and discussion

5.1 Comparison of the domain adaptation effect

As shown in Fig. 4, the best cluster number (k) in the clustering algorithm was selected according to the Calinski–Harabasz (CH) index. The CH index is the ratio of the sum of between-cluster dispersion and within-cluster dispersion for all the clusters, and the dispersion is defined as the sum of distances squared [9]. A high CH index implies that the clusters are dense and well separated. Then, the k values determined based on the highest CH index in the CA1 calibration of Cases 1–3 were 4 and in the CA2 calibration of Cases 1–3 were 5, 6, and 4, respectively.

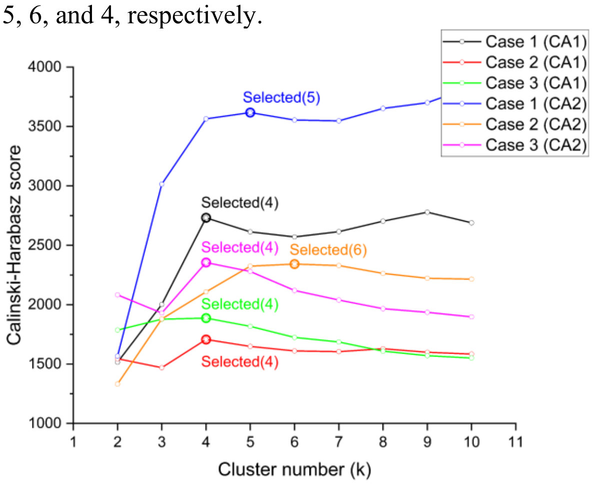

Fig. 4. Selection results of cluster numbers for clustering.

For CA1 calibration, the wind speed ranges of the source and target data were 0.2–9.7 and 0.2–8.2 m/s, respectively, with a difference of 1.5 m/s. Although this difference was insignificant, the features between the source and target data were not yet recognized and matched. After domain adaptation based on clustering, the results of Tables 3(a-1) and (a-2) described that the difference between the wind speed ranges of divided CA's source and target data in some clusters reduced. For example, the wind speed ranges of the source and target data in cluster 2 were 0.2–4.4 and 0.2–4.0 m/s, with a difference of 0.4 m/s. This is conducive to building a more accurate ANN model. Most importantly, Cases 2 and 3 can better separate the data acquired using the CA at the OS* location than Case 1, as the source and target data in cluster 4 more precisely exhibit the same lowest wind speed range.

For CA2 calibration, the wind speed ranges of the source and target data were 0.1–10.4 and 0.2–7.8 m/s, respectively, with a difference of ~2.7 m/s. Moreover, the results in Tables 3(b-1) and (b-2) represent that the difference in the wind speed ranges between the source and target data was reduced in some clusters. Based on the highest k value of Case 2, the differences in the wind speed ranges between the source and target data in clusters 1–6 were 2.6, 0.6, 0.6, 0.6, 3.0, and 0.1 m/s. Specifically, Case 2 effectively separates CA's data at the BS* location, as its source and target data in cluster 6 exhibit almost the same lowest wind speed range. Cases 1–3 can align the wind speed range of source and target data in varying degrees, and Case 2 performs well at the OS* and BS* locations.

Table 3. Wind speed ranges (m/s) of divided CA's 10-min-interval data series in each cluster after applying domain adaptation based on clustering with different feature selections.

(a-1) Divided source data (OS)

Cluster	Case 1	Case 2	Case 3
1	582 (0.2–9.7)	769 (0.2–9.7)	652 (0.2–9.7)
2	712 (0.2–6.9)	705 (0.2–4.4)	796 (0.2–6.2)
3	485 (0.2–6.2)	324 (0.2–6.2)	350 (0.2–3.7)
4	151 (0.2–0.6)	132 (< 0.2)	132 (< 0.2)

(a-2) Divided target data (OS*)

Cluster	Case 1	Case 2	Case 3
1	28 (0.2–8.0)	45 (0.2–8.2)	38 (0.2–8.2)
2	78 (0.2–8.2)	82 (0.2–4.0)	87 (0.2–4.3)
3	36 (0.2–5.1)	15 (0.2–3.6)	17 (0.2–1.7)
4	4 (< 0.2)	4 (< 0.2)	4 (< 0.2)

(b-1) Divided source data (BS)

Cluster	Case 1	Case 2	Case 3
1	220(0.2–10.4)	237(0.2–10.4)	245(0.2–10.4)
2	592 (0.1–6.4)	310 (0.1–6.2)	907 (0.1–6.2)
3	400 (0.1–6.2)	497 (0.1–4.1)	None
4	281 (0.1–4.8)	415 (0.1–3.3)	345 (0.1–4.8)
5	None	86 (0.2–4.8)	None
6	437 (0.1–1.0)	385 (0.1–0.4)	433 (0.1–0.8)

(b-2) Divided target data (BS*)

Cluster	Case 1	Case 2	Case 3
1	6 (0.2–7.3)	11 (0.2–7.8)	13 (0.2–7.8)
2	77 (0.2–7.8)	32 (0.2–5.7)	162 (0.2–5.7)
3	108 (0.2–5.5)	94 (0.2–3.6)	None
4	57 (0.2–2.8)	119 (0.2–2.8)	71 (0.2–2.8)
5	None	1 (0.2–1.4)	None
6	43 (0.2–0.7)	34 (0.2–0.4)	45 (0.2–0.8)

5.2 Evaluation index on calibration results

As the error evaluation of the instantaneous wind speed values of regression prediction results, four indexes (coefficient of determination (R^2), mean absolute error (MAE), root mean squared error (RMSE), and symmetric mean absolute percentage error (SMAPE)) listed in Table 4 were used. R^2 can reflect the goodness of fit between the instantaneous CA and UA values, whereas the MAE and RMSE focus on measuring the deviation between the instantaneous CA and UA values. As such, the quantification of error involved the same order of magnitude as the data, and the latter is more sensitive to outliers because it contains the squared value of the error. Compared with the RMSE, SMAPE demonstrates the average relative percentage error and is more robust, as the errors are normalized.

Table 4. Error evaluation index along with their lower and upper bounds (LB and UB). $u(t)$, $\bar{u}(t)$, and $\hat{u}(t)$ denote true data series, mean of data series, and predicted data series.

Index	Formula	LB	UB	0 error
R^2	$1-\frac{\sum_{t=1}^{n}\left(u(t)-\hat{u}(t)\right)^2}{\sum_{t=1}^{n}\left(u(t)-\bar{u}(t)\right)^2}$	$-\infty$	1	1
MAE	$\frac{1}{n}\sum_{t=1}^{n}\lvert u(t)-\hat{u}(t)\rvert$	0	∞	0
RMSE	$\sqrt{\frac{1}{n}\sum_{t=1}^{n}\left(u(t)-\hat{u}(t)\right)^2}$	0	∞	0
SMAPE	$\frac{1}{n}\sum_{t=1}^{n}\frac{\lvert u(t)-\hat{u}(t)\rvert}{(\lvert u(t)\rvert+\lvert \bar{u}(t)\rvert)/2}$	0	∞	0

The wind speed statistics (Mean, Max, STD, TI, and GF) are evaluated in each 10-min-interval data series to compare the pulsation parameters of the calibrated and CA and UA values. Then, relative errors (E) of the aforementioned statistics defined in Eq. (1) are applied to characterize calibration accuracy.

$$E=\frac{\lvert e_t-\hat{e}_t\rvert}{e_t}\times 100\%. \tag{1}$$

In the aforementioned equation, e_t denotes the wind speed statistic evaluated by UA's 10-min-interval data series, and $\hat{e}_t$ indicates the wind speed statistic evaluated based on the CA's 10-min-interval data series and calibrated 10-min-interval data series.

5.3 Comparison of calibration accuracy

The R^2, MAE, RMSE, and SMAPE results of all the cases are listed in Table 5. There was a reduction in the measurement inaccuracy of the CA with regard to instantaneous wind speed. Cases 2 and 0 exhibited the best effects in the OS* and BS* locations, and other cases have also achieved similar calibration accuracy.

The relative errors (E) of the wind speed statistics in each 10-min-interval data series were compared among all the cases (Table 6). In the OS* location, the mean and median values of E_{STD} and E_{TI} of Case 2 were minimum. In the BS* location, the median and mean values of E_{max}, E_{STD}, E_{TI}, and E_{GF} of Case 2 were minimum.

Overall, the calibration accuracy of Case 2 outperformed other cases, specifically in the recovery of the wind speed fluctuation characteristics. At the corner (side) of the building, for Case 2, the average relative errors of STD, TI, and GF reduced more by ~2% (8%), ~3% (7%), and ~1% (1%), respectively, than that of the conventional machine learning method (Case 0). The calibrated and noncalibrated mean wind speed and turbulence intensity values are summarized in Fig. 5.

The results indicated that the overestimated TI based on CA measurements significantly improved, and the calibration effect of Case 2 was better than other cases. Studies to overcome the difficulty of CA calibration in the low wind domain, which is below the start-up wind speed (0.5 m/s in this study), to recover more wind pulsation characteristics will be considered in the future.

Table 5. Error evaluation of non-calibrated and calibrated CA measurements. (Bold font represents the lowest error.)

(a) OS* location

Metric	Calibration cases for CA				
	None	Case 0	Case 1	Case 2	Case 3
R^2 (-)	0.922	0.979	**0.981**	**0.981**	**0.981**
MAE (m/s)	0.221	0.105	0.104	**0.102**	**0.102**
RMSE (m/s)	0.288	0.148	0.144	**0.141**	0.142
SMAPE (-)	0.289	0.152	0.144	**0.141**	0.142

(b) BS* location

Metric	Calibration cases for CA				
	None	Case 0	Case 1	Case 2	Case 3
R^2 (-)	0.789	**0.920**	0.916	0.917	0.915
MAE (m/s)	0.244	**0.158**	0.160	**0.158**	0.159
RMSE (m/s)	0.315	**0.194**	0.199	0.197	0.199
SMAPE (-)	0.504	**0.296**	0.303	0.302	0.301

Table 6. Mean (Median) of the relative error evaluation of 10-min-interval wind speed statistics by multi-calibration cases. (Bold font represents the lowest error.)

(a) OS* location

Statistics	Calibration cases for CA				
	None	Case 0	Case 1	Case 2	Case 3
E_{mean} (%)	14.9 (10.6)	5.1 (1.8)	**4.8 (1.8)**	5.0 (1.9)	5.1 (2.0)
E_{max} (%)	10.1 (6.6)	5.0 (2.8)	5.5 (2.7)	5.1 (2.9)	**5.0 (2.7)**
E_{STD} (%)	13.0 (6.6)	9.7 (3.9)	9.1 (3.5)	**8.1 (3.5)**	8.3 (3.5)
E_{TI} (%)	25.9 (17.5)	12.1 (4.6)	10.4 (4.1)	**9.0 (4.5)**	9.2 (4.6)
E_{GF} (%)	11.4 (5.6)	6.3 (2.5)	4.9 (2.4)	4.9 (2.6)	**4.8 (2.4)**

(b) BS* location

Statistics	Calibration cases for CA				
	None	Case 0	Case 1	Case 2	Case 3
E_{mean} (%)	27.3 (23.9)	**17.1 (9.6)**	19.5 (9.8)	18.8 (10.1)	19.2 (9.2)
E_{max} (%)	20.3 (13.5)	13.0 (11.7)	12.5 (11.1)	**11.8 (10.6)**	12.2 (11.0)
E_{STD} (%)	23.9 (9.3)	27.8 (16.8)	21.4 (13.4)	**19.5 (12.4)**	20.9 (13.5)
E_{TI} (%)	47.1 (37.6)	24.5 (11.0)	20.9 (8.3)	**18.0 (6.7)**	20.0 (8.5)
E_{GF} (%)	26.5 (18.5)	12.2 (5.1)	11.8 (5.9)	**11.1 (5.4)**	11.8 (6.0)

6 Conclusion

To achieve efficient data-driven calibration of the CAs, this study proposes a method of transfer learning based on domain adaptation. It uses existing measurement data for model training in new measurement scenarios to reduce the cost of secondary training data collection. Domain adaptation was achieved based on the feature-based clustering analysis for matching the source and target data in each cluster. As a result, the calibration effect of the proposed method was superior to the conventional machine learning method. Overall, in two locations, i.e., the corner and side of a 15-m-high building of a new measurement site, the results of Case 2 confirmed more reduction in the relative errors of most pulsation parameters, e.g., standard deviation wind speed, turbulence intensity, and gust factor compared to the conventional machine learning method. In addition, based on the comparative study of three different feature selections for clustering analysis, it was found that the appropriate choice with five features (Mean, TI, Max, STD, and GF of instantaneous wind speed in the 10-min-interval data series) mainly improved the calibration accuracy.

References

[1] Siebert, H., & Teichmann, U. Behaviour of an ultrasonic anemometer under cloudy conditions. Boundary-Layer Meteorology, 94(1), 165–169 (2000).
[2] Kristensen, L. Cup anemometer behavior in turbulent environments. Journal of Atmospheric and Oceanic Technology, 15(1), 5–17 (1998).
[3] Bisignano, A., Carotenuto, F., Zaldei, A., & Giovannini, L. Field calibration of a low-cost sensors network to assess traffic-related air pollution along the Brenner highway. Atmospheric Environment, 275, 119008 (2022).
[4] Bégin-Drolet, A., Lemay, J., & Ruel, J. Time domain modeling of cup anemometers using artificial neural networks. In Flow Measurement and Instrumentation, 33, 10–27 (2013).
[5] Rongmao Li, Hideki Kikumoto, Data-driven calibration of cup anemometer based on field measurements and artificial neural network for wind measurement around buildings, Journal of Wind Engineering and Industrial Aerodynamics, 231 (2022).
[6] Panigrahi, S., Nanda, A., & Swarnkar, T. A Survey on Transfer Learning. Smart Innovation, Systems and Technologies, 194(10), 781–789 (2021).
[7] Sophian, A, Tian, GY, Taylor, D, & Rudlin, J. A feature extraction technique based on principal component analysis for pulsed Eddy current NDT. NDT & E International, 36, 37–41 (2003).
[8] Joe H. Ward Jr. Hierarchical Grouping to Optimize an Objective Function, Journal of the American Statistical Association, 58:301, 236-244 (1963).
[9] T. Caliński & J Harabasz. A dendrite method for cluster analysis, Communications in Statistics, 3:1, 1-27 (1974).

 https://doi.org/10.1051/e3sconf/202339605016

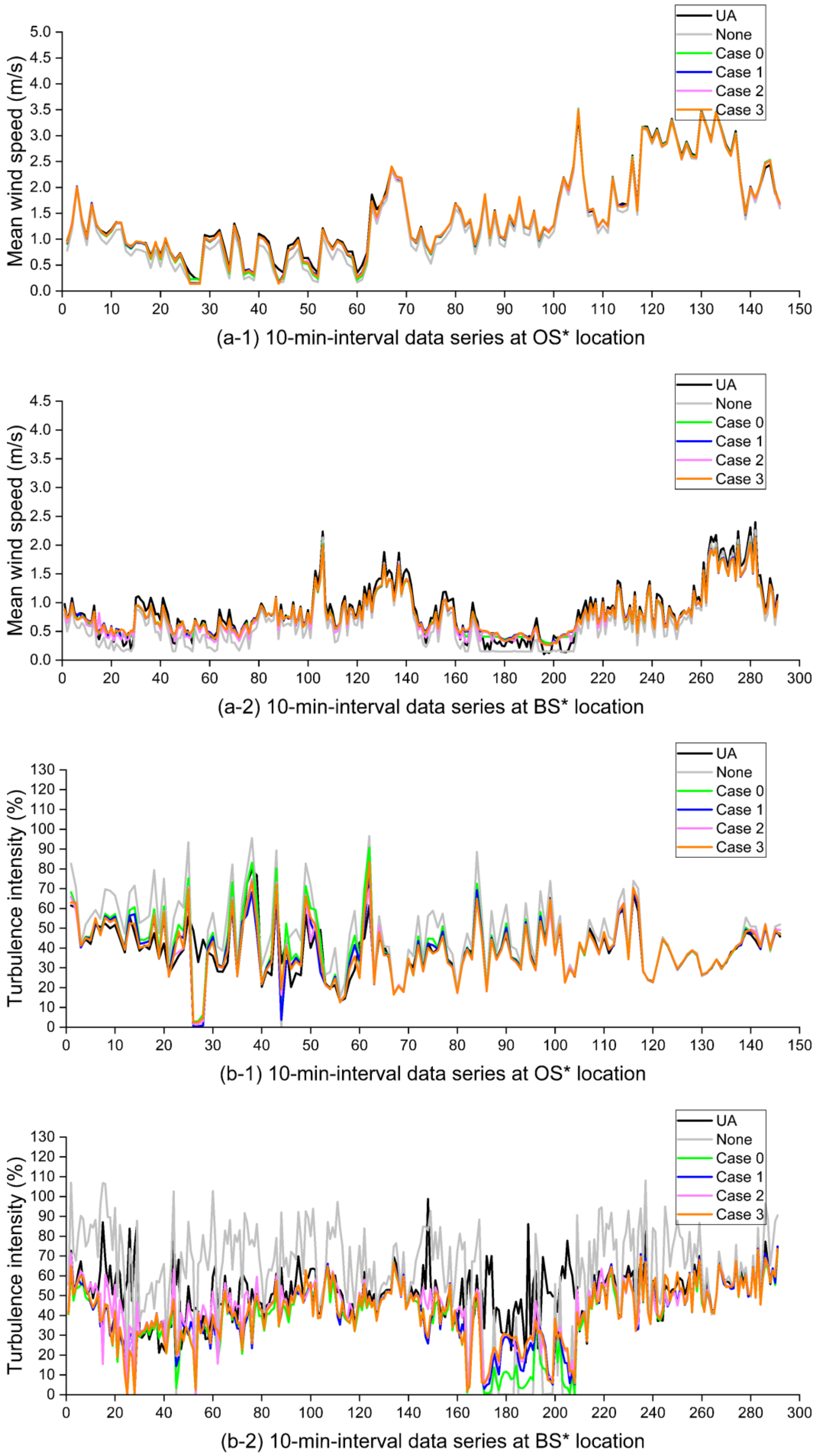

Fig. 5. Comparison of the mean (a-1, a-2) and TI (b-1, b-2) values after applying calibration.